Effect of the herbal formulation Jianpijiedu on the TCRVβCDR3 repertoire in rats with hepatocellular carcinoma and subjected to food restriction combined with laxative

BAOGUO SUN*, JUN MENG*, TING XIANG, LEI ZHANG, LIUXIANG DENG, YAN CHEN, HAOXUAN LUO, ZHANGBIN YANG, ZEXIONG CHEN and SHIJUN ZHANG

Department of Traditional Chinese Medicine, The First Affiliated Hospital of Sun Yat-Sen University, Guangzhou, Guangdong 510080, P.R. China

Received November 4, 2014; Accepted November 5, 2015

DOI: 10.3892/etm.2015.2955

Abstract. The aim of this study was to investigate the effects of the Chinese herbal formulation Jianpijiedu (JPJD) in a rat model of orthotopic hepatocellular carcinoma (OHC). The tumor-bearing rats underwent food restriction combined with laxative (FRL) treatment in order to model the nutritional and digestive symptoms of patients with hepatocellular carcinoma. In addition, the study aimed to elucidate the effect of JPJD on the T cell receptor Vβ-chain complementarity-determining region 3 (TCRVβCDR3) repertoire and the underlying mechanism. The FRL rat model was established by alternate-day food restriction and the oral administration of Glauber's salt (sodium sulfate), based on which the OHC model was then established. Subsequently, the FRL-OHC induced animals received JPJD or thymopentin-5 (TP5) for 17 days. Differences in the TCRVβCDR3 repertoire in the rat thymus, liver and hepatocellular carcinoma tissues were analyzed by polymerase chain reaction. Compared with the FRL-OHC model animals without any treatment, those treated with JPJD exhibited significantly inhibited hepatocellular carcinoma growth ($P<0.05$), reduced weight loss ($P<0.01$) and stable visceral indices ($P<0.05$). Furthermore, the JPJD treatment appeared to improve Simpson's diversity index (Ds) values and the quasi-Gaussian distribution rate of the TCRVβCDR3 repertoire in the thymus, liver and hepatocellular carcinoma tissues. However, no anti-hepatoma effects were evident in the rats treated with TP5. In addition, TP5 increased the Ds values and the quasi-Gaussian distribution rate of the TCRVβCDR3 repertoire in hepatocellular carcinoma tissues compared with those in the JPJD-treated group. The anti-hepatoma effects of JPJD in FRL-OHC-induced animals may be due to the promotion of the Ds values of the TCRVβCDR3 repertoire.

Correspondence to: Professor Zexiong Chen or Professor Shijun Zhang, Department of Traditional Chinese Medicine, The First Affiliated Hospital of Sun Yat-Sen University, Zhongshan 2nd Road, Guangzhou, Guangdong 510080, P.R. China
E-mail: zexiong333@163.com
E-mail: zhsjun1967@hotmail.com

*Contributed equally

Key words: hepatocellular carcinoma, food restriction, laxative, T cell receptor Vβ-chain complementarity-determining region 3

Introduction

The Chinese herbal formulation Jianpijiedu (JPJD), also known as Fuzheng Jiedu, has been proposed as a complementary therapy for the treatment of hepatocellular carcinoma due to its ability to enhance the absorption and transportation of nutrients and to reduce tumor burden. A randomized clinical trial of patients with hepatocellular carcinoma has shown that this formulation can effectively promote quality of life and liver function if combined with intra-arterial chemotherapy (1). Furthermore, studies have indicated that JPJD can improve survival time, reduce pulmonary metastasis (2) and maintain the body and visceral weight of nude mice transplanted with human hepatocellular carcinoma tissue (3). These previous findings indicate that JPJD may be able to improve digestive and absorptive functions and the quality of life in patients with hepatocellular carcinoma.

Decreased food intake and diarrhea are common clinical symptoms in patients with hepatocellular carcinoma, and may lead to compromised immunity, acceleration of tumor growth and nutrient deprivation (4-6). Differences in the expression of T cell receptor Vβ-chain complementarity-determining region 3 (TCRVβCDR3), which indicates the status of cell-mediated immunity, occur rapidly following the immunological recognition of endogenous and exogenous antigens by the immune system in malignant tumors (7-9). However, few studies have investigated the changes in the TCRVβCDR3 repertoire in hepatocellular carcinoma.

In the present study, a food restriction combined with laxative (FRL) rat model was established by alternate-day food restriction (10,11) and the oral administration of Glauber's salt (sodium sulfate; Na_2SO_4) (12). The purpose of this was to model the nutritional and digestive symptoms of

patients with hepatocellular carcinoma, which include diarrhea, vomiting and anepithymia, and are relevant to a loss of immune function. On the basis of this, the orthotopic hepatocellular carcinoma (OHC) model was established (13,14). Subsequently, the FRL-OHC-model animals received JPJD or thymopentin-5 (TP5) treatment. Differences in the TCRVβCDR3 repertoires in the thymus, liver and hepatocellular carcinoma tissues of the rats were analyzed to elucidate the immunological mechanism underlying the anti-hepatoma effects of JPJD.

Materials and methods

Experimental animals and cell lines. This study was performed at the Medical Science Experimentation Center of the Zhongshan School of Medicine of Sun Yat-Sen University (Guangzhou, China). Male specific pathogen-free (SPF) Lewis rats (age, 3-4 weeks; weight, 70±15 g) were purchased from the Beijing Vital River Laboratory Animal Technology Co., Ltd. (Beijing, China). Male SPF BALB/c nude rats (age, 4-6 weeks; weight, 15±2 g) were purchased from the Guangdong Medical Laboratory Animal Center (Guangzhou, China). All animals were housed according to the national animal treatment guidelines (http://www.gov.cn/gongbao/content/2011/content_1860757.htm) and all experimental procedures were approved by the Committee on the Use of Live Animals for Teaching and Research of Sun Yat-Sen University and the Ethics Committee of the First Affiliated Hospital of Sun Yat-Sen University [Approval no. Ethical application (2013) No. 149]. The Walker 256 cell line was acquired from the Cell Bank of the Laboratory Center of Sun Yat-Sen University. Glauber's salt (Guangzhou Pharmaceuticals Corporation, Guangzhou, China) containing 99.0% Na_2SO_4 was dissolved in ultraviolet (UV)-disinfected saline to a concentration of 2 g/ml.

Medicinal reagents. A Glauber's salt solution was prepared, as described above. Concentrated JPJD cream was prepared, which was composed of 30 g *Codonopsis* (root), 15 g *Poria*, 15 g *Atractylodes* (root), 6 g liquorice (*Glycyrrhiza glabra)*, 12 g *Bupleurum* (root) 15 g *Curcuma* (root) and 30 g *Scutellaria barbata* (stem and leaf), which were obtained from China Resources Sanjiu Medical & Pharmaceutical Co., Ltd., Beijing, China). The sources, which were identified according to the first part of the 1998 Chinese Pharmacopoeia and combined according to the established ratio (12), were concentrated using water extraction and volatile oil collection. These procedures were performed at the Science and Technology Industrial Park of Guangzhou University of Chinese Medicine (Guangzhou, China). Finally, the JPJD formulation was diluted into a concentrated aqueous cream that contained 2 g crude components per ml. TP5 solution (10 mg; license no. H20058462; cat no. 20130806; Beijing ShuangLu Pharmaceutical Co., Ltd., Beijing, China) was utilized for injection.

Devices and reagents. TRIzol® reagent (15596-026; Thermo Fisher Scientific, Shanghai, China); polymerase chain reaction (PCR) amplification kit (DR011; Takara Biotechnology Co., Ltd., Dalian, China); Hi-Di Formamide (Lot no. 1305031; serial no. 4404307), GeneScan™ 600 LIZ® (Lot no. 1206023; serial no. 4408399) and an Applied Biosystems 3500xL Genetic Analyzer (Thermo Fisher Scientific); and GeneMarker® Genotyping software, version 2.2 (SoftGenetics LLC, State College, PA, USA) were used.

Primer sequences for TCRVβCDR3 analysis. The primer sequences were as reported in a previous study by Douillard *et al* (15). They were synthesized using an ABI 3900 desktop high-throughput DNA synthesizer (Thermo Fisher Scientific).

Study design. Male Lewis rats (age, 3-4 weeks), which were housed under a temperature of 24-26˚C at a 12-h light/dark cycle, were randomized into five groups (n=15 per group) as follows: i) Control group (group A), animals received 1 ml/100 g normal saline per day intragastrically; ii) FRL-OHC group (group B), animals received treatment to establish the FRL-OHC model; iii) low dose JPJD group (group C), animals received treatment to establish the FRL-OHC model and the intragastric administration of 37.5 g/kg JPJD per day; iv) high dose JPJD group (group D), animals received treatment to establish the FRL-OHC model and the intragastric administration of 75 g/kg JPJD per day; and v) TP5 group (group E), animals received treatment to establish the FRL-OHC model, an intramuscular injection of 5 mg TP5 every 48 h and 1 ml/100 g normal saline per day intragastrically. All rats were fed simultaneously. The FRL model establishment procedure was terminated for animals in groups B-E after 29 days. Following 7 days of free feeding, the OHC model was then established in the relevant groups. Similarly, there was 17 days of free feeding and observation. Liver, thymus and hepatocellular carcinoma samples were collected under anesthesia immediately after the rats with OHC reached the ethical limits for animal experimentation (lethargy, erect back hair, relative body mass of 80%, fever or ascites). Anesthesia was induced via an intraperitoneal injection of 10% chloral hydrate (3.5 ml/kg; Sigma-Aldrich Shanghai Trading Co., Ltd., Shanghai, China). Samples were stored at -80˚C prior to analysis. Apparent FRL scale scores and body mass were recorded daily in each group. Hepatocellular carcinoma volume was calculated as follows: Maximal diameter (mm) x minimal diameter $(mm)^2/2$. Visceral indices were calculated as follows: Weight of the cancer-bearing liver or thymus (g) or hepatocellular carcinoma volume x 100/final body weight (g). Following the completion of the study, three rats from each group were selected and their thymus, liver and hepatocellular carcinoma tissues were harvested from the anesthetized rats to analyze the spectral-type diversity of TCRVβCDR3 repertoire. For group A, the three rats were selected at random, while for the other groups, three rats with a maximal hepatocellular carcinoma diameter ≥10 mm were selected from each group.

Establishment of the FRL model. Rats were housed individually at 23±1˚C with a 12-12 h light-dark cycle and a feeding regimen of tap water *ad libitum* and alternate-day food restriction (11). Rats received food between 9:00 a.m. one day to 9:00 a.m. the following day. For the following 24 h, the rats received water only. The rat diet accorded with the National

Table I. Evaluation of the apparent indices of the food restriction combined with laxative model.

	Grading			
Index	1	2	3	4
Relative body mass (%)	≥95	90-94	85-89	<85
Mental state	Normal	Irritable	Lethargic	Somnolent
Chill or fever	Normal	Curled up	Chill	Arched back, trembling
Breathing	Normal	Panting	Dyspnea	Faint
Hair	Normal	Matted	Fluffy erect hair	Brown erect hair
Feces	Normal	Loose	Wet and loose	Mucous

Standard of China, and consisted of water (10%), crude protein (18%), crude fat (4%), crude fiber (5%), crude ash (8%), calcium (1.2%) and phosphorus (1%). For each feeding period, 200 g food was administered and the remaining food was measured on the next day to calculate the food intake per 100 g body mass. Glauber's salt solution (0.25 g/ml) (12) was administered daily (1 ml/100 g) via oral gavage for 29 days prior to feeding. The effect of the FRL modeling was evaluated according to the apparent FRL scale (Table I) based on factors including the degree of weight loss, tail cleanliness and hair color and aggregation.

In the apparent FRL model scale, the grading criterion for relative body mass was developed according to the limitation of 20% human weight loss (16). During the establishment of the FRL model, rats in groups A and B were matched according to weight (weight difference, ±5 g) for calculation of the relative body mass (FRL rat weight/normal rat weight as a percentage). During the period of FRL-OHC model establishment, the rats were 8-9 weeks old and their weight gain reduced, thus another equation was required: Relative body mass = final weight/weight prior to establishment of the model. A total score of ≤6 on the apparent FRL model scale was considered to be asymptomatic, 7-12 was mildly symptomatic, 13-18 was typically symptomatic and 19-24 was severely symptomatic.

Establishment of the OHC model. The OHC model was established according to previously described procedures (13,14). In brief, Walker-256 cells ($1x10^7$) were transplanted subcutaneously by an injection made in the neck of nude BALB/c rats. Tumors were harvested after reaching a diameter of >1 cm. First, the animals were anesthetized via an intraperitoneal injection of 10% chloral hydrate (3.5 ml/kg; Sigma-Aldrich Shanghai Trading Co., Ltd., Shanghai, China), then the thoracic and abdominal cavities were opened and the tissues or organs were carefully removed. Following the removal of necrotic tissue, the tumor tissues were cut into 1-mm^3 pieces. The tissue fragments were then implanted into the FRL model Lewis rats to establish the OHC model. Under inhalation anesthesia, a vertical incision under the xiphoid was cut after sterilization. Inhalation anesthesia was induced as follows: 4 ml ether (Tianjin Damao Chemical Reagent Factory, Tianjin, China) were transferred to a 15-ml centrifuge tube (Becton Dickinson Medical Devices, Shanghai, Co Ltd, Shanghai, China) and a cotton ball (Winner Medical Co. Ltd., Shenzhen, China) was added and left to soak. Following soaking, the cotton ball was moved close to the nose of the animal inducing anesthesia. The anesthetic procedure lasted for a maximum of 3 min. Subsequently, the liver of the rat was exposed and cancer tissues were implanted using a 1-mm coarse needle (Cat. no. 305198; Becton Dickinson Medical Devices Shanghai Co., Ltd., Shanghai, China). Finally, the abdominal cavity was closed layer by layer after hemostasis was achieved.

Detection of TCRVβCDR3 repertoire. Total RNA extraction, PCR analysis and TCRVβCDR3 repertoire detection were performed according to methods described by Douillard *et al* (15) and Venturi *et al* (17). An ABI 3500xL Genetic Analyzer was used for fragment analysis of the TCRVβCDR3 repertoire according to the manufacturer's instructions (18).

TCRVβCDR3 type analysis. TCRVβCDR3 fragment analysis data obtained using the ABI 3500xL and GeneScan™ 600 LIZ® was imported into GeneMarker software, version 2.2 (19). The spectral diagram and related data of the 20 gene fragments of the TCRVβCDR3 subfamily were obtained.

Data analysis of the TCRVβCDR3 repertoire. The diversities of the TCRVβCDR3 repertoire in the thymus, liver and cancerous tissues in each group were compared with the normal repertoire diversity and fragment sizes in the thymus tissue in the control group (17,20). Fluorescence peaks and their data that did not correspond to the sites of the various TCRVβCDR3 subfamilies of the normal thymus tissue were deleted to retain comparability between the groups.

Clonal types of the TCRVβCDR3 subfamily were confirmed visually by three independent researchers. The normal spectral-type of the TCRVβCDR3 subfamilies is a bell-shaped quasi-Gaussian distribution; however, other non-Gaussian distributions may appear, including a skewed-peak type, a no clonal type (no peak detected) and a monoclonal type (one peak detected).

Three samples were analyzed for each group. The results indicated that for each group, the TCRVβCDR3 subfamily spectral-types, expressed and unexpressed, of the thymus, liver and cancerous tissues of the three samples were identical. During data analysis, the number of the TCRVβCDR3 subfamilies, expressed and unexpressed, was used as the

Table II. Apparent food restriction combined with laxative (FRL) scale scores.

Group	Apparent FRL scale score
A	4.45±2.65[a]
B	16.97±5.24
C	17.37±4.33
D	16.88±7.04
E	16.55±7.23

[a]P<0.001 vs. groups B, C, D and E (one-way analysis of variance). Values are presented as mean ± standard deviation (n=15 per group).

raw data. Medians of the numbers of the fluorescence peaks and clonal types (quasi-Gaussian distribution, skewed-peak and monoclonal type) were used, while means of Simpson's diversity index (Ds), area under the fluorescence peak and relative fluorescence intensity of the each peak were used for the analysis. The relative fluorescence intensity (RI) was determined using the following formula: RI (%) = (100 x area under the fluorescence peak of the target fragment)/(total area under the fluorescence peak of the complete subfamily). In the calculations, the area under the fluorescence peak was expressed as $1x10^{-3}$ of the original value, and the Ds value was expressed as 100-fold of the original value. As these data involved only three samples, they were not analyzed using statistical tests.

Statistical analysis. Data were analyzed using SPSS software, version 17.0 (SPSS, Inc., Chicago, IL, USA). Continuous measurement data were expressed as the mean ± standard deviation. Analysis of variance was used for the normally distributed measurement data. Rank sum tests and Kaplan-Meier survival analysis were used for the non-normally distributed measurement data. P<0.05 was considered to indicate a statistically significant difference.

Results

General condition of the animals

Apparent FRL scale scores. The apparent FRL scale scores of the animals in each group are presented in Table II. The apparent FRL scale score of the animals in group A was <6 due to normal feeding without any intervention, while the scores of the rats in groups B, C, D and E indicated that their symptoms were moderate or severe.

Anatomical indices and differences in body weight. The anatomical indices and changes of body weight are presented in Table III. An evident reduction in body weight gain was observed due to FRL model establishment. The hepatocellular carcinoma volume (with the exception of group A) and the hepatic and thymus indices of the animals were observed to be similar in groups A, C and D, and reduced compared with those in groups B and E. The body weight gain was significantly increased in group A compared with the other groups. In the rats subjected to OHC modeling, the body weight loss of the rats in group B was the greatest while the body weight loss of the rats in groups D and E was the lowest among the groups.

Hepatocellular carcinoma growth. The growth states of representative hepatocellular carcinoma on day 17 in each group are presented in Fig. 1.

Spectral-type diversity of the TCRVβCDR3 repertoire

Overview of the repertoire diversity of the TCRVβCDR3 subfamily. A total of 20 TCRVβCDR3 subfamily repertoires were obtained from the normal thymus tissue and 19 from the normal liver tissue. Fragment sizes varied between 100 and 250 bp, and had a quasi-Gaussian distribution (a normal or bell-shaped distribution). FRL, OHC and FRL-OHC model establishment factors reduced the number of subfamily clonal types, expression of fragments, diversity of the TCRVβCDR3 repertoire and the Gaussian distribution rate, and increased the skewed-peak and monoclonal types.

Expression of TCRVβCDR3 clonal types in the thymus, liver and cancer tissues. The TCRVβCDR3 subfamilies V1, V2, V4, V6, V8, V11, V13, V15, V17 and V18 were expressed in all the three tissues types in all the groups. By contrast, the subfamily V7 was expressed in the thymus tissue of group A, but not in the other tissues of the control group or in any of the tissues in groups B, C, D and E.

In total, there were 8 TCRVβCDR3 subfamilies that were not expressed in the thymus tissue, and 13 not expressed in the liver tissue (group E > group D = group B > group C > group A). V3 was not expressed in groups C, D or E, while V16 was not expressed in groups B, D or E. However, there was a total of 18 unexpressed TCRVβCDR3 subfamilies in the cancer tissue (group B > group C = group D > group E). V3 was not expressed in groups B, C or E while V10 and V16 were not expressed in groups B, C or D (Table IV).

Numbers of TCRVβCDR3 subfamily fragments expressed in the thymus, liver and hepatocellular carcinoma tissues. The total peak numbers indicated that TCRVβCDR3 diversity was the greatest in the thymus tissue, followed by the liver tissue and the hepatocellular carcinoma tissue. Specifically, the numbers of TCRVβCDR3 subfamily fragments in the various tissues were as follows: Thymus tissue, group A > group C > group D > group E > group B; liver tissue, group A > group D > group C > group E > group B; and hepatocellular carcinoma tissue, group E > group D > group C > group B (Table V).

Analysis of TCRVβCDR3 repertoire diversity in the thymus, liver and hepatocellular carcinoma tissues

TCRVβCDR3 repertoire Ds values in thymus, liver and hepatocellular carcinoma tissues. The TCRVβCDR3 repertoire Ds values in the thymus and liver tissues of group A were the highest among the groups. Additionally, in group A the thymus tissues exhibited an increased Ds value compared with the liver tissues. The Ds values of TCRVβCDR3 subfamily repertoires in the various tissues were ranked as follows: Thymus tissue, group A > group C = group D > group E > group B; liver tissue, group A > group D > group C > group E > group B; and hepatocellular carcinoma tissue, group E > group D > group C > group B (Table VI).

Comparison of TCRVβCDR3 clonal types in the thymus, liver and hepatocellular carcinoma tissues. The percentages of

Table III. Viscera index and changes in body weight during model establishment (mean ± standard deviation).

Group	Hepatocellular carcinoma volume index (mm^3/g)	Hepatic index	Thymus index	Body weight change	
				FRL model	OHC model
A	-	3.62±0.30	0.09±0.03	68.42±7.93	58.25±10.66
B	2.28±0.48[a]	4.20±0.80[a]	0.10±0.02	14.25±11.35[b]	-19.25±11.79[b]
C	1.77±0.64	3.86±0.34	0.09±0.02	12.33±15.64[b]	-6.17±8.61[b,c]
D	1.76±1.49	3.74±0.30	0.09±0.02	13.80±21.44[b]	-2.2±2.95[b-d]
E	2.22±0.59[a]	4.21±0.49[a]	0.10±0.02	14.75±11.47[b]	-3.25±8.88[b-d]

[a]P<0.05 vs. group C and D; [b]P<0.01 vs. group A; [c]P<0.01 vs. group B; [d]P<0.01 vs. group C. FRL, food restriction combined with laxative; OHC, orthotopic hepatocellular carcinoma.

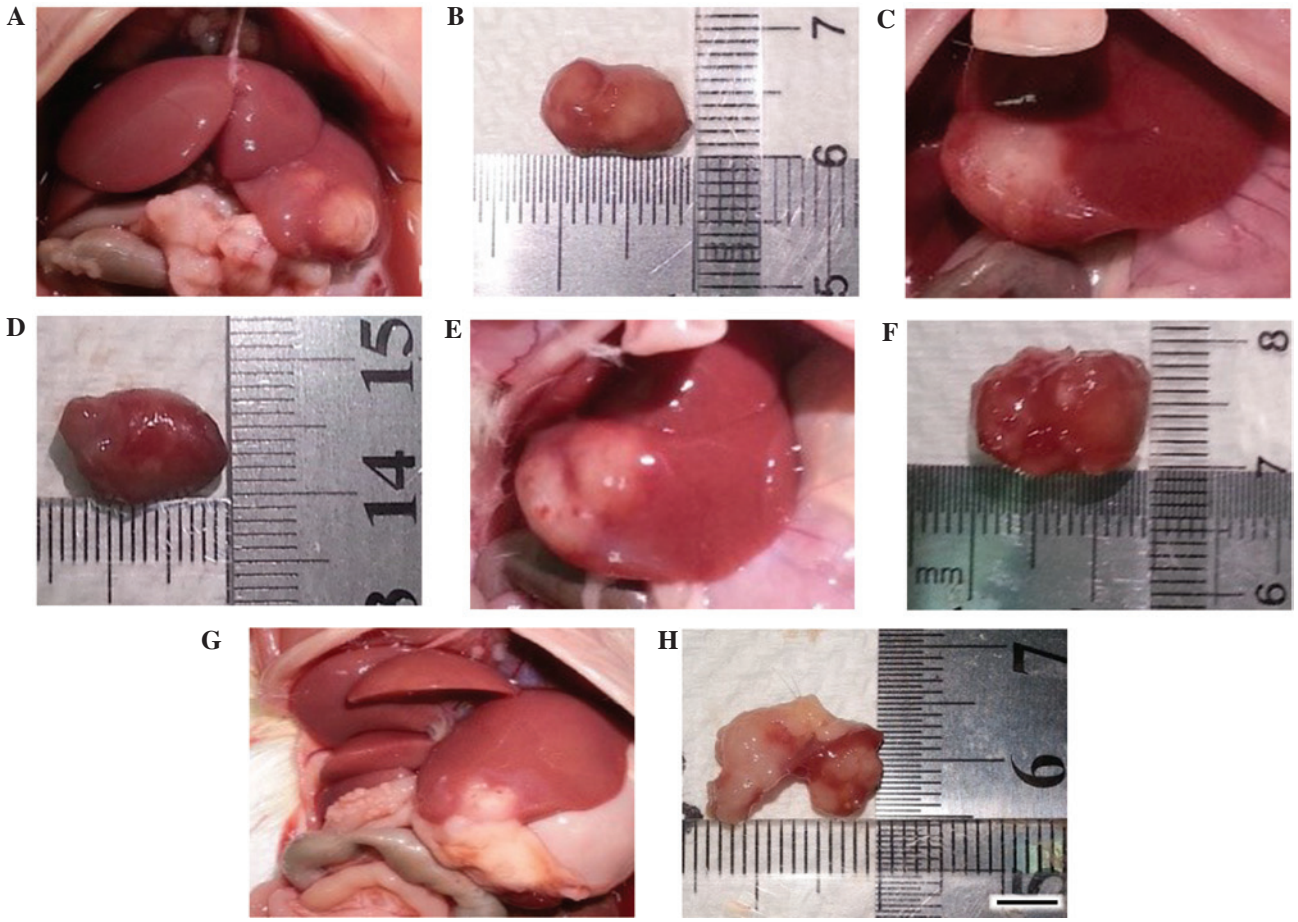

Figure 1. Growing states of hepatocellular carcinoma on day 17 in each group. (A, C, E and G) The exposed livers and (B, D, F and H) the respective isolated tumors. The hepatocellular carcinoma exhibited vigorous growth by day 17, with a diameter of ~1 cm. Compared with (A and B) the untreated group B, Jianjipiedu significantly inhibited the growth of hepatocellular carcinoma tissues in (C and D) group C and (E and F) group D (P<0.05). (G and H) In the rats in group E, thymopentin-5 did not produce a significant difference in tumor size compared with that in group B (scale bar, 50 mm).

TCRVβCDR3 clonal types fitting a quasi-Gaussian distribution ranked as follows: Thymus tissue, group A > group C = group D > group E > group B; liver tissue, group A > group E > group D > group C > group B; and hepatocellular carcinoma tissue, group D > group E > group C > group B. The skewed-peak distributions were as follows: Thymus tissue, group B > group E > group A = group C = group D; liver tissue, group D > group E > group C > group A > group B; and hepatocellular carcinoma tissues, group B > group E > group C = group D. The monoclonal types were as follows: Thymus tissues, group B > group E > group C = group D = group A; liver tissues, group B > group C > group E > group D > group A (Table VII).

Areas under the shared TCRVβCDR3 subfamily fluorescence peaks and maximal RI values of all subfamilies of the thymus, liver and hepatocellular carcinoma tissues. Table VIII shows

Table IV. Unexpressed TCRVβCDR3 subfamilies.

Group	Thymus	Liver	Cancer
A	None	**V7**	-
B	**V7**, V12, V14, V19, V20	V5, **V7**, **V16**	**V3**, V5, **V7**, V9, V10, **V16**
C	**V7**	**V3**, **V7**	**V3**, **V7**, V10, V12, **V16**
D	**V7**	**V3**, **V7**, **V16**	**V7**, V9, V10, **V16**, V20
E	**V7**	**V3**, **V7**, V12, **V16**	**V3**, V7

Bold font represents the shared-unexpressed TCRVβCDR3 subfamilies. TCRVβCDR3, T cell receptor Vβ-chain complementarity-determining region 3.

Table V. Number of TCRVβCDR3 subfamily fluorescence peaks (median).

	Thymus					Liver					Cancer			
Subfamily	A	B	C	D	E	A	B	C	D	E	B	C	D	E
V1	12	2	9	7	7	3	1	2	1	2	1	1	2	6
V2	11	7	8	10	8	7	2	3	4	5	3	5	6	6
V3	11	3	9	6	4	5	2	0	0	0	0	0	4	0
V4	11	5	8	7	8	7	4	1	3	5	4	4	4	6
V5	11	6	9	8	8	7	0	3	4	2	0	3	5	7
V6	9	8	8	9	7	5	1	4	4	3	3	5	5	7
V7	8	0	0	0	0	0	0	0	0	0	0	0	0	0
V8	12	7	9	9	8	9	6	5	4	3	3	3	6	6
V9	11	5	9	9	9	5	1	4	2	1	0	1	0	3
V10	13	1	7	7	7	8	3	2	3	3	0	0	0	5
V11	13	3	7	7	8	6	1	1	3	1	1	2	3	3
V12	11	0	7	7	1	3	1	3	2	0	1	0	3	5
V13	10	1	7	8	8	5	1	3	2	2	2	2	5	6
V14	10	0	9	7	7	6	5	5	4	2	2	5	4	7
V15	13	1	8	7	7	6	5	3	6	4	8	5	5	4
V16	10	1	7	7	6	8	0	1	0	0	0	0	0	4
V17	11	1	8	7	5	5	5	5	4	5	3	3	4	4
V18	11	1	9	8	9	6	4	3	5	2	4	3	6	6
V19	9	0	8	7	8	7	1	1	4	2	2	2	1	6
V20	13	0	8	7	8	5	1	1	3	3	3	2	0	6
Total	220	52	154	144	133	113	44	50	58	45	40	46	63	97

TCRVβCDR3, T cell receptor Vβ-chain complementarity-determining region 3.

that the areas under the shared TCRVβCDR3 subfamily fluorescence peaks were ranked as follows: Thymus tissues, group A > group C > group E > group D > group B; liver tissues, group A > group D > group E > group C > group B; and hepatocellular carcinoma tissues, group E > group D > group C > group B. The maximal RI values of all the subfamilies were ranked as follows: Thymus tissues, group B > group E > group D > group C > group A; liver tissues, group B > group C > group E > group D > group A; and hepatocellular carcinoma tissues, group B > group C > group D > group E.

Discussion

According to the theory of traditional Chinese medicine, JPJD exerts certain effects, including enhancement of the absorption and transportation of nutrient substances and an antitumor effect (2). However, previous studies have indicated that JPJD can effectively promote quality of life and survival time, but is not able to directly inhibit tumor growth (2,3). Therefore, a hepatocellular carcinoma model based on food restriction combined with laxative (FRL) administration was established in the present study in order

Table VI. Comparison of Ds in each group (mean ± standard deviation).

Group	Thymus	Liver	Hepatocellular carcinoma
A	95.35±1.29	95.23±0.59	-
B	91.55±1.28	93.45±0.71	92.56±0.99
C	95.31±1.29	94.94±0.58	94.01±0.93
D	95.31±1.26	95.04±0.56	94.06±0.94
E	95.08±1.33	94.55±0.61	95.12±0.99

Data multiplied by 100 based on the original data.

Table VII. TCRVβCDR3 subfamily clonal types as evaluated using the visual method, n (%).

	Quasi-Gaussian distribution			Skewed-peak distribution			Monoclonal type	
Group	Thymus	Liver	Hepatocellular carcinoma	Thymus	Liver	Hepatocellular carcinoma	Thymus	Liver
A	20 (100.0)	8 (42.11)	-	0 (0.00)	11 (57.89)	-	0 (0.00)	0 (0.00)
B	5 (33.33)	2 (11.77)	2 (14.29)	4 (26.67)	7 (41.18)	9 (64.29)	6 (40.00)	8 (47.06)
C	19 (100.0)	3 (16.67)	6 (40.00)	0 (0.00)	11 (61.11)	7 (46.67)	0 (0.00)	4 (22.22)
D	19 (100.0)	3 (17.65)	7 (46.67)	0 (0.00)	13 (76.47)	7 (46.67)	0 (0.00)	1 (5.89)
E	15 (78.95)	3 (18.75)	8 (44.44)	3 (15.79)	11 (68.75)	10 (55.56)	1 (5.26)	2 (12.50)

TCRVβCDR3, T cell receptor Vβ-chain complementarity-determining region 3.

Table VIII. Total areas under the shared TCRVβCDR3 subfamily fluorescence peaks[a] and maximal RI values of all subfamilies.

	Thymus		Liver		Hepatocellular carcinoma	
Group	Area	RI	Area	RI	Area	RI
A	6,539.42±2,325.22	25.54±2.64	1,238.38±438.79	37.30±11.05	-	-
B	37.71±29.44	62.39±34.44	33.35±30.35	69.04±31.28	34.99±28.52	63.88±24.48
C	817.60±155.43	27.99±4.20	47.86±18.69	61.85±26.07	56.10±22.23	56.36±22.64
D	332.44±98.89	28.05±5.06	67.17±31.63	50.77±19.59	72.75±32.92	53.90±20.51
E	479.34±198.84	34.96±16.61	56.76±38.88	56.16±22.78	104.55±62.34	37.96±12.06

[a]Twenty-four unexpressed subfamilies were excluded. Values are presented as mean ± standard deviation (n=3 per group). TCRVβCDR3, T cell receptor Vβ-chain complementarity-determining region 3; RI, relative fluorescence intensity.

to investigate the immunological mechanism underlying the potential anti-hepatoma effects of JPJD with TCRVβCDR3 as the suggested target.

FRL-OHC model establishment was observed to significantly inhibit the body weight gain of the rats, leading to a compensatory increase of the viscera and the proliferation of hepatocellular carcinoma. The JPJD treatment appeared to maintain the body weight and viscera in a normal state and inhibit the proliferation of hepatocellular carcinoma, while treatment with TP5 alone did not. JPJD and TP5 were individually able to alleviate the body weight reduction in FRL-OHC model animals.

The analysis of unexpressed TCRVβCDR3 subfamilies indicated that almost all TCRVβCDR3 subfamilies were expressed in the normal thymus and liver tissues. The numbers of TCRVβCDR3 subfamilies expressed in the thymus, liver and hepatocellular carcinoma tissues were significantly reduced by FRL-OHC modeling, and increased by the JPJD and TP5 treatments. Furthermore, JPJD increased the number of expressed TCRVβCDR3 subfamilies more markedly compared with TP5 in the liver tissues, while TP5 increased them to a greater extent in the hepatocellular carcinoma tissues.

FRL-OHC model establishment significantly reduced the numbers of fragments, Ds values and areas under the

shared TCRVβCDR3 subfamily fluorescence peaks in the thymus, liver and hepatocellular carcinoma tissues, and these effects were attenuated by the JPJD and TP5 treatments. Specifically, JPJD increased the number of fragments, Ds values and area under the shared TCRVβCDR3 subfamily fluorescence peaks to a greater extent than did TP5 in the liver tissues, whereas TP5 increased these parameters more markedly in the hepatocellular carcinoma tissues.

A Gaussian distribution of T cells represents the normal situation in healthy individuals, whereas a skewed-peak distribution is indicative of an abnormality, such as immunoinflammatory condition, or clonal hyperplasia due to the stimulating effect of a tumor (20). Analysis of the clonal distributions in the present study indicated that JPJD and TP5 treatments significantly improved the quasi-Gaussian distribution rate of the TCRVβCDR3 subfamilies in the FRL-OHC model animals, and the effects of the JPJD were more marked compared with those of TP5. In addition, regarding the polyclonal skewed-peak type distribution, JPJD and TP5 increased the skewed-peak distribution of TCRVβCDR3 subfamilies in the liver tissues, while reducing it in the hepatocellular carcinoma tissues. Furthermore, JPJD reduced the monoclonal rates of TCRVβCDR3 subfamilies to a greater extent compared with TP5 in the liver and thymus tissues. Similarly, the ability of JPJD to lower the RI value was higher compared with that of TP5 in the thymus tissues, while the RI value-lowering effect of TP5 was higher compared with that of JPJD in the hepatocellular carcinoma tissues.

Total areas under the shared TCRVβCDR3 subfamily fluorescence peaks were highest in the control group thymus tissues, while the RI values in these tissues were the lowest (25.54±2.64%) amongst all the groups. The results indicated that TCRVβCDR3 subfamily fluorescence peaks have a bell-shaped distribution in a normal situation. By contrast, the total areas under the shared TCRVβCDR3 subfamily fluorescence peaks declined in the FRL-OHC model rats, with an increased RI value and a loss of the Gaussian distribution, which was normalized by the JPJD and TP5 treatments.

In conclusion, the effects of JPJD and TP5 in the treatment of the FRL-OHC model animals and the diversity of the TCRVβCDR3 repertoire were as follows. High-dose JPJD (75 g/kg) exhibited an improved effect compared with that of the low-dose JPJD (37.5 g/kg) treatment. Furthermore, the effect of JPJD on the FRL-OHC model rats was improved compared with that of TP5; however, further studies are recommended in order to elucidate the specific mechanism underlying the effects of JPJD and TP5 on the diversity of the TCRVβCDR3 repertoire. TP5 is an immune-regulating drug that functions by stimulating the maturation and differentiation of T cells, and has been well utilized as a complementary therapy for the treatment of hepatocellular carcinoma (21-26). In the present study, TP5 appeared to alter the diversity of the TCRVβCDR3 repertoire; however, the underlying mechanism and clinical value of this effect require further study.

Acknowledgements

This research was supported by grants from the National Natural Science Foundation of China for Young Scholars (grant no. 81102581), the National Natural Science Foundation of China (grant no. 81373500) and the Administration of Traditional Chinese Medicine of Guangdong Province (grant no. 20141046).

References

1. Chen ZX, Zhang SJ, Hu HT, Sun BG and Yin LR: Clinical study of method of strengthening body resistance and disintoxication in patients with HCC of post-TACE. Zhongguo Zhong Yao Za Zhi 32: 1211-1213, 2007 (In Chinese).
2. Yin LR, Chen ZX, Zhang SJ, Sun BG, Liu YD and Huang HZ: Expression of phosphatase and tensin homolog deleted on chromosome ten in liver of athymic mice with hepatocellular carcinoma and the effect of Fuzheng Jiedu Decoction. World J Gastroenterol 14: 108-113, 2008.
3. Sun B, Meng J, Xiang T, Chen Z, Li Y, Lu L, Zhang S and Chen X: Jianpijiedu fang improves survival of hepatocarcinoma mice by affecting phosphatase and tensin homolog, phosphoinositide 3-kinase and focal adhesion kinase. J Tradit Chin Med 33: 479-485, 2013.
4. Taylor AK, Cao W, Vora KP, De La Cruz J, Shieh WJ, Zaki SR, Katz JM, Sambhara S and Gangappa S: Protein energy malnutrition decreases immunity and increases susceptibility to influenza infection in mice. J Infect Dis 207: 501-510, 2013.
5. Finn OJ: Cancer Immunology. N Engl J Med 358: 2704-2715, 2008.
6. Valdés-Ramos R and Benítez-Arciniega AD: Nutrition and immunity in cancer. Br J Nutr 98 (Suppl 1): S127-S132, 2007.
7. Zhang M, Maiti S, Bernatchez C, Huls H, Rabinovich B, Champlin RE, Vence LM, Hwu P, Radvanyi L and Cooper LJ: A new approach to simultaneously quantify both TCR α- and β-chain diversity after adoptive immunotherapy. Clin Cancer Res 18: 4733-4742, 2012.
8. Wang QJ, Hanada K, Feldman SA, Zhao Y, Inozume T and Yang JC: Development of a genetically-modified novel T-cell receptor for adoptive cell transfer against renal cell carcinoma. J Immunol Methods 366: 43-51, 2011.
9. Kim JA, Rao P, Graor H, Rothchild K, O'keefe C and Maciejewski JP: CDR3 spectratyping identifies clonal expansion within T-cell subpopulations that demonstrate therapeutic antitumor activity. Surgery 136: 295-302, 2004.
10. Islam S, Abély M, Alam NH, Dossou F, Chowdhury AK and Desjeux JF: Water and electrolyte salvage in an animal model of dehydration and malnutrition. J Pediatr Gastroenterol Nutr 38: 27-33, 2004.
11. Duarte FO, Sene-Fiorese M, Cheik NC, Maria AS, de Aquino AE Jr, Oishi JC, Rossi EA, Garcia de Oliveira Duarte AC and Dâmaso AR: Food restriction and refeeding induces changes in lipid pathways and fat deposition in the adipose and hepatic tissues in rats with diet-induced obesity. Exp Physiol 97: 882-894, 2012.
12. Editorial Committee of Chinese Herbs, State Administration of Traditional Chinese Medicine of the People's Republic of China. A Selection of Chinese Herbal Medicines. Vol I. Shanghai Science and Technology Press, Shanghai, pp57-60, 1998 (In Chinese).
13. Gong LS, Zhang YD and Liu S: Target distribution of magnetic albumin nanoparticles containing adriamycin in transplanted rat liver cancer model. Hepatobiliary Pancreat Dis Int 3: 365-368, 2004.
14. Chen JH, Ling R, Yao Q, Wang L, Ma Z, Li Y, Wang Z and Xu H: Enhanced antitumor efficacy on hepatoma-bearing rats with adriamycin-loaded nanoparticles administered into hepatic artery. World J Gastroenterol 10: 1989-1991, 2004.
15. Douillard P, Pannetier C, Josien R, Menoret S, Kourilsky P, Soulillou JP and Cuturi MC: Donor-specific blood transfusion-induced tolerance in adult rats with a dominant TCR-Vbeta rearrangement in heart allografts. J Immunol 157: 1250-1260, 1996.
16. Fearon K, Strasser F, Anker SD, Bosaeus I, Bruera E, Fainsinger RL, Jatoi A, Loprinzi C, MacDonald N, Mantovani G, *et al*: Definition and classification of cancer cachexia: An international consensus. Lancet Oncol 12: 489-495, 2011.
17. Venturi V, Kedzierska K, Turner SJ, Doherty PC and Davenport MP: Methods for comparing the diversity of samples of the T cell receptor repertoire. J Immunol Methods 321: 182-195, 2007.

18. Kirkham A, Haley J, Haile Y, Grout A, Kimpton C, Al-Marzouqi A and Gill P: High-throughput analysis using AmpFlSTR® Identifiler® with the Applied Biosystems 3500xl Genetic Analyzer. Forensic Sci Int Genet 7: 92-97, 2013.
19. Hulce D, Li X, Snyder-Leiby T and Johathan CS Liu: GeneMarker® Genotyping Software: Tools to Increase the Statistical Power of DNA Fragment Analysis. J Biomol Tech 22 (Suppl): S35-S36, 2011.
20. Lu J, Basu A, Melenhorst JJ, Young NS and Brown KE: Analysis of T-cell repertoire in hepatitis-associated aplastic anemia. Blood 103: 4588-4593, 2004.
21. Goldstein G and Audhya TK: Thymopoietin to thymopentin: Experimental studies. Surv Immunol Res 4 (Suppl 1): 1-10, 1985.
22. Reggiani PC, Morel GR, Cónsole GM, Barbeito CG, Rodriguez SS, Brown OA, Bellini MJ, Pléau JM, Dardenne M and Goya RG: The thymus-neuroendocrine axis: Physiology, molecular biology and therapeutic potential of the thymic peptide thymulin. Ann NY Acad Sci 1153: 98-106, 2009.
23. Wang Y, Ke XY, Khara JS, Bahety P, Liu S, Seow SV, Yang YY and Ee PL: Synthetic modifications of the immunomodulating peptide thymopentin to confer anti-mycobacterial activity. Biomaterials 35: 3102-3109, 2014.
24. Petronella P, Ferrone R, Freda F and Valeriani G: Thymopentin and immune response in patients with cancer. Minerva Chir 44: 2017-2020, 1989 (In Italian).
25. Li T, Li ZW and Wen HC: Study on the efficacy and safety of high dose thymopentin combined with trans-artery chemoembolization for primary liver cancer. Zhonghua Zhong Liu Za Zhi 29: 941-942, 2007 (In Chinese).
26. Li J, Cheng Y, Zhang X, Zheng L, Han Z, Li P, Xiao Y, Zhang Q and Wang F: The in vivo immunomodulatory and synergistic anti-tumor activity of thymosin α1-thymopentin fusion peptide and its binding to TLR2. Cancer Lett 337: 237-247, 2013.